

In Vivo Splenic Clearance Correlates with *In Vitro* Deformability of Red Blood Cells from *Plasmodium yoelii*-Infected Mice

Sha Huang,^{a,b} Anburaj Amaladoss,^c Min Liu,^c Huichao Chen,^d Rou Zhang,^c Peter R. Preiser,^{c,f} Ming Dao,^{c,e} Jongyoon Han^{a,b,g}

Department of Electrical Engineering and Computer Science, Massachusetts Institute of Technology, Cambridge, Massachusetts, USA^a; Biosystems and Micromechanics IRG, Singapore-MIT Alliance for Research and Technology, Singapore^b; Infectious Diseases IRG, Singapore-MIT Alliance for Research and Technology, Singapore^c; Department of Biostatistics, Harvard School of Public Health, Boston, Massachusetts, USA^d; Department of Materials Science and Engineering, Massachusetts Institute of Technology, Cambridge, Massachusetts, USA^e; School of Biological Sciences, Nanyang Technological University, Singapore^f; Department of Biological Engineering, Massachusetts Institute of Technology, Cambridge, Massachusetts, USA^g

Recent experimental and clinical studies suggest a crucial role of mechanical splenic filtration in the host's defense against malaria parasites. Subtle changes in red blood cell (RBC) deformability, caused by infection or drug treatment, could influence the pathophysiological outcome. However, *in vitro* deformability measurements have not been directly linked *in vivo* with the splenic clearance of RBCs. In this study, mice infected with malaria-inducing *Plasmodium yoelii* revealed that chloroquine treatment could lead to significant alterations to RBC deformability and increase clearance of both infected and uninfected RBCs *in vivo*. These results have clear implications for the mechanism of human malarial anemia, a severe pathological condition affecting malaria patients.

The spleen serves as the largest filter of blood in the human body by initiating immune responses against blood-borne microorganisms and removing abnormal blood cells (1). Two major structural features of the spleen enable its critical functions: the white pulp (including the marginal zone), which contains the majority of immune effector cells, and the red pulp, a reticular meshwork that filters abnormal red blood cells (RBCs) (2). In humans, 76 to 79% of the spleen is made of red pulp, a dense meshwork composed of splenic cords and splenic sinuses. Previous studies on different animal (dog, cat, and rat) models revealed that from 90% (3–5) to 10% (6) of total splenic blood undergo so-called “closed circulation,” during which RBCs traverse venous sinuses bypassing the red pulp; open circulation occurs in the remaining blood, whereby RBCs enter the reticular meshwork, following slow microcirculation (1, 7). The structural and mechanical quality of the RBCs is ascertained by the mechanical constraint imposed by the meshwork in the red pulp, where old and abnormal RBCs that are less deformable are retained and eventually removed by phagocytosis (7).

The important implications of RBC deformability in the pathogenesis of malaria have been extensively discussed (8–13). A significant decrease in RBC deformability arising from *Plasmodium falciparum* invasion was observed *in vitro* with different measurement techniques, including optical tweezers (9), micropipette aspiration (13), RBC membrane fluctuations (i.e., diffraction phase microscopy) (12), and probing of cells under flow (i.e., microfluidic flow cytometry) (10). Such parasitization of RBCs has been shown to increase their stiffness manifold, with their elimination by mechanical filtration expected to compromise their microcirculation (8).

The connection between RBC deformability and splenic clearance has been demonstrated in a series of *ex vivo* spleen studies (7, 14–17). Splenic retention of both ring-stage malaria-infected RBCs (iRBCs) and artificially hardened (17) (by heating) uninfected RBCs (uRBCs) was observed *ex vivo* perfusion of human spleen (14). It is evident that, besides possible molecular interactions, the mechanical properties of RBCs play a vital role in the

process of splenic RBC clearance. This was further validated by experiments that mimicked splenic retention *in vitro* using a microsphere filtration system (16).

In fact, the role of the spleen in influencing the pathogenesis of malaria has been well documented in a number of clinical studies. Splenomegaly (enlarged spleen) is a characteristic clinical consequence of malaria infection, and therefore, the size of the spleen has been used to estimate the intensity of malaria transmission (2). Clinical studies involving radioactively labeled RBCs revealed that patients with an enlarged spleen display a more rapid clearance of RBCs than patients with a normal spleen (18). It has been proposed that splenomegaly modifies blood microcirculation and splenic filterability (2). Studies on splenectomized hosts that show higher fatality rates and delayed parasite clearance after antimalarial treatment (19) also point to the role of the spleen in the clinical outcomes for malaria patients.

Experiments also suggest that splenic retention of RBCs could contribute to malarial anemia (17), which is a common consequence of severe malaria associated with high mortality (20). Excessive splenic clearance of RBCs is considered a likely mechanism for malarial anemia (17). However, removal of only the iRBCs cannot be the primary cause of such massive blood loss (20), particularly since clinical studies do not find a correlation between severe malarial anemia and a high parasitemia level in the patient

Received 2 December 2013 Returned for modification 27 January 2014

Accepted 24 March 2014

Published ahead of print 31 March 2014

Editor: J. H. Adams

Address correspondence to Jongyoon Han, jghan@mit.edu, or Ming Dao, mingdao@mit.edu.

Supplemental material for this article may be found at <http://dx.doi.org/10.1128/IAI.01525-13>.

Copyright © 2014, American Society for Microbiology. All Rights Reserved.

doi:10.1128/IAI.01525-13

(21, 22). These observations suggest the possibility that excessive clearance of uRBCs could play a key role in the development of malarial anemia. While this process is not fully understood, several mechanisms have been proposed for the increased clearance of uRBCs, including the activation of splenic macrophages and enhanced splenic mechanical retention by altering the mesh size of spleen red pulp (20).

How antimalarials influence RBC retention in the spleen could consequently impact the outcomes of malaria therapy; however, the mechanical impact of chloroquine (CQ) on host RBCs has not been explored. In the past, the inhibition of hemozoin formation was inferred as a key mechanistic consequence of chloroquine treatment (23). Hemozoin is a nontoxic crystal synthesized by the parasites as they digest RBC hemoglobin (Hb) and release highly toxic (ferriprotoporphyrin IX) α -hematin (24). Since hematin may lead to RBC membrane disruption and eventually host cell lysis (25), the parasites need to convert hematin to hemozoin for their own survival. It is known that CQ can prevent hematin polymerization (23), but whether it also modifies host RBC deformability and consequently alters splenic RBC retention is unknown.

Although *ex vivo* studies (14) of human spleen show retention of both iRBCs and artificially hardened uRBCs, little is known about the RBC splenic clearance during the course of malaria infection and antimalarial treatment. Furthermore, a better understanding from *in vivo* studies of possible connections between the mechanical retention of RBCs in the spleen and excessive blood loss or anemia is needed. The dynamic splenic response interweaves host, parasite, and antimalarial drugs in such a complex manner that *ex vivo* spleen studies alone are insufficient to predict the role of splenic retention in influencing any anemic response in the host. Therefore, a quantitative and more direct measurement of the deformability of both spleen minced blood (SMB) (see “Animal preparation” below) and peripheral venous blood (PVB) in healthy and malaria-infected host is highly desirable.

The rodent malarial model has been commonly used to complement the research on *Plasmodium falciparum* (20, 26). Splenic clearance of parasitized RBCs was determined to play an important role in both humans (17) and mice (27). In this study, we identified *Plasmodium yoelii* as the most relevant rodent model to study *in vivo* splenic RBC clearance, for it shares similar invasion characteristics (28) with *Plasmodium falciparum*. Careful consideration was also given to the structural similarities and differences between human and mouse spleens. Human spleen is sinusoidal (29); human RBCs (8 μm) have to squeeze through the interendothelial slits ($\sim 1 \mu\text{m}$) (16) in venous sinus walls, which act as a mechanical filter to abnormal or stiffened RBCs (5). In comparison, though mouse spleen is arguably classified as nonsinusoidal (5), the fenestrations in the walls of mouse pulp venules are so small (1 to 3 μm) (30) compared to murine RBCs ($\sim 6 \mu\text{m}$) that they still function just like venous sinus and mechanically trap less-deformable RBCs (31).

To assess the deformability of RBCs in mouse spleen, we extracted mouse RBCs from both PVB and SMB and quantitatively evaluated the deformability of the RBCs using a microfluidic deformability cytometer (10). Several important aspects relating to splenic RBC retention were explored: first, we established the correlation between the *in vitro* deformability assay and *in vivo* splenic retention; second, the effects of malaria infection and/or antimalarial drug treatment on RBC deformability as well as on splenic RBC retention were investigated; and third, we attempted

to use 2 different approaches to estimate the splenic retention threshold based on RBC deformability. Physically, the retention threshold is decided by the effective pore size of the reticular meshwork or the splenic slits, as well as the RBC geometry (size and shape) and membrane stiffness. In this study, we estimated the retention threshold below which RBCs are considered to be most likely retained, expressed as a fraction of normalized PVB velocity. Finally, the possible anemic effect related to increased splenic retention, in both infected and uninfected mice and with or without drug treatment, was investigated.

MATERIALS AND METHODS

Murine model for malaria infection. Four- to six-week-old male or female BALB/c mice were infected with 1×10^5 parasites of *Plasmodium yoelii* YM by intraperitoneal (i.p.) injection. Blood smears from these infected mice showed 1 to 10% parasitemia at approximately 4 days postinfection. Mice were then injected with drug or phosphate-buffered saline (PBS) for 3 consecutive days by i.p. injection as described below.

Microfluidic deformability measurement. The deformability of single RBCs was assessed using a microfluidic deformability cytometer (see Fig. S1B in the supplemental material) as described previously (10). Blood samples were diluted to 0.1 to 1% hematocrit before loading to the system to minimize cell-cell interactions. The system was operated in pressure-driven mode. RBC movement in the main channel was captured by a charge-coupled device (CCD) camera and the video could be postanalyzed using ImageJ software. The deformability for every RBC was characterized by its average traverse velocity across repeated bottleneck structures. The device channel height is 4.2 μm which ensures white blood cells and other cells from splenic minced blood to stay in the reservoir and not enter the main channel. However, we note that due to the extremely complex cell mixtures in spleen minced sample (especially from the infected mice), device throughput is limited. In the present study, we still managed to measure a reasonable sample size, which are larger than other conventional RBC deformability measurement methods such as micropipette aspiration or optical tweezers, for all conditions.

Animal preparation. Adult BALB/c mice each weighing approximately 20g were used for our experiments. Four treatment conditions were included: healthy mice/saline, healthy mice/CQ, malaria-infected mice/saline, and malaria-infected mice/CQ. Prior to the experiments, approximately 10 μl venous blood was taken from all mice for baseline measurements for both RBC deformability studies and Hb assays. During the experiments, the healthy mice were bled (approximately 10 μl) on alternating days and the malaria-infected mice were bled only on the first and the last experimental days. The spleens of all mice were harvested when they were culled. Spleens were minced with sterile scissors and forceps. The extracted blood was washed three times before being loaded to the device.

Drug treatment. Chloroquine diphosphate salt (Sigma-Aldrich) was dissolved in deionized (DI) water at a final concentration of 100 mM and stored at -20°C freezer. A working dose was then prepared weekly by diluting the stock solution with $1 \times \text{PBS}$ at a ratio of 2:11 and stored at 4°C . The mice received 100 μl diluted CQ solution daily via i.p. injection. In the control groups, mice were injected with 100 μl sterile PBS solution. Three consecutive days of CQ or saline treatments were carried out for all malaria-infected mice, and their spleens were harvested. For healthy mice, the drug effect was studied over CQ treatment days. Mice received 4, 6, or 8 days of consecutive CQ or saline injection before being culled on the following day (see Fig. S1A in the supplemental material).

Sample preparation. To differentiate iRBCs from uRBCs, Hoechst dye (33342; Sigma) was added to the sample 20 min prior to the microfluidic flow cytometry experiment so that the infected cells were fluorescent under UV excitation. A fixed interpillar gap size of 3 μm was used for all mouse RBC deformability measurements to achieve the best deformation differentiation. The microfluidic device is precoated with 1% bovine

serum albumin (BSA) (or 20% fetal bovine serum [FBS]) to minimize confounding effects due to RBC adhesion.

Experimental flow chart. The deformability of RBCs was investigated in uninfected or *P. yoelii* (YM)-infected BALB/c mice. Figure S1A in the supplemental material shows the flow chart for one experimental round, consisting of 6 healthy mice and 6 *P. yoelii* infected mice. At least three experimental rounds were performed to achieve sufficient mouse and cell counts for all characterizations (including microfluidic deformability, microscopy morphology, micropipette aspiration, hemoglobin assay, and spleen mass and size quantification). For the experiments involving only healthy mice, three of them received 750 μg (i.e., approximately 30 mg/kg) of chloroquine (CQ) via intraperitoneal (i.p.) injection daily (32, 33) and were therefore referred as healthy/drug mice. The remaining three healthy mice received an equal volume of $1\times$ phosphate-buffered saline (PBS) solution and were termed healthy/control mice. On experimental day 1, approximately 10 μl of blood was extracted from all healthy mice to establish baseline measurement. After 4 consecutive days of CQ or PBS treatment, one mouse each from the healthy/control and healthy/drug groups was culled on day 5. Both peripheral venous blood (PVB) and splenic minced blood (SMB) (34) were collected for subsequent measurement. CQ and PBS treatment continued for the remaining four healthy mice, and the procedure was repeated on days 7 and 9 until all mice were culled. For the experiments involving infected mice, 10^5 parasites of *P. yoelii* YM were injected in all 6 mice at 2 to 3 days prior to the experiment. The parasitemia was monitored by Giemsa-stained thin blood smear every 24 h. When parasite levels first reached $>1\%$ for all infected mice, 10 μl blood was taken for baseline measurement (i.e., experimental day 1). At this stage, three infected mice received CQ drug treatment (the malaria/drug group), and the remaining three mice received a PBS placebo (the malaria/control group) for 3 consecutive days. All mice were culled on day 4, and the PVB and SMB were collected. At this stage the malaria/drug mice had an average parasitemia of less than 1%, while the malaria/control mice had an average parasitemia of 50 to 90%. It is noted that more than three experimental rounds were carried out to ensure data reproducibility among different animals and to achieve sufficient data points for statistical analysis. All studies involving mice were approved by the Institutional Animal Care and Use Committee (IACUC) of the National University of Singapore and Committee on Animal Care (CAC) of the Massachusetts Institute of Technology.

Statistical testing. The two-tailed Mann-Whitney test was used for *P* value computations unless otherwise specified.

RESULTS

Splenic RBC retention based on RBC deformability profiles. RBC deformability profiles were characterized with a cell deformability cytometer, a microfluidic device which consists of triangular pillar arrays as described by Bow et al. (10) (see Fig. S1B in the supplemental material). The interpillar gap size was selected to be 3 μm for all mouse RBC measurements. Individual RBCs deformed considerably as they passed through the device, and their traverse velocities were recorded to describe a population-wide deformability profile (Fig. 1A and B). It is understood that a higher traverse velocity corresponds to higher deformability (10, 11, 13). The deformability (velocity) profiles of RBCs sampled from PVB were compared to those of RBCs from SMB of the same mice. As the red pulp of the spleen is capable of retaining the abnormal and hardened RBCs, a fraction of splenic minced RBCs was attributable to the splenic trapped RBCs, while the remainder would represent healthy, normally circulating RBCs (34). Therefore, two significant RBC subpopulations in the splenic minced RBCs were assumed: (i) “flowthrough” RBCs that share very similar mechanical properties with the peripheral RBCs and (ii) abnormal or senescent RBCs that were trapped in the splenic meshwork (16, 35). Mathematically the population wide splenic RBC

velocity profile can be expressed as follows: $V_{\text{SMB}} = (1 - a_1)V_{\text{PVB}} + a_1V_{\text{trapped}}$, where V_{SMB} , V_{PVB} , and V_{trapped} represent the average deformabilities (or velocities) of SMB, flowthrough, and splenic trapped RBCs, respectively, and a_1 denotes the fraction of SMB that came from spleen-trapped cells. Comparison of the normalized SMB velocity against the average velocity of the PVB sample of the same healthy mouse (Fig. 1A) showed that the RBC velocity of SMB was on average 15% lower than that of PVB ($P < 0.001$), reflected as a very gentle left shift in the velocity histogram (Fig. 1B). This difference in blood deformability profiles was likely contributed by the second subpopulation in SMB samples, reflecting the fraction (i.e., a_1) of less-deformable RBCs trapped in the splenic meshwork. No significant difference in the size distributions of PVB and SMB RBC populations was identified (see Fig. S7 in the supplemental material).

A similar analysis was also performed on *P. yoelii*-infected mice, and the infected RBCs (iRBCs) were differentiated from uninfected RBCs (uRBCs) by Hoechst staining (36). Figure 1C illustrates different deformability profiles of both uRBCs and iRBCs extracted from SMB and PVB samples. The average uRBC and iRBC velocities in SMB were, respectively, 21% and 30% lower than those of the uRBCs and iRBCs in the PVB ($P < 0.001$). Splenic sequestration of less-deformable RBCs is one likely explanation (15). The reduced splenic iRBC velocity reconciled with the increased membrane shear modulus analyzed by micropipette aspiration (see Fig. S10 in the supplemental material). The more pronounced difference between PVB and SMB in the infected mice (21% and 30%, compared to 10% in healthy mice, according to microfluidic velocity profiles) indicates a possibly increased splenic retention in mice after *P. yoelii* infection. This was further supported when examining the sizes of the healthy and *P. yoelii* infected mice spleens, as it has been demonstrated clinically that splenomegaly is linked with enhanced RBC clearance in spleen (17, 18, 37): the length of an infected mouse spleen (Fig. 1E) was approximately 1.6 times that of a healthy mouse spleen (i.e., $\sim 4\times$ volume enlargement), suggesting that a more intense RBC clearance is likely to have occurred. The deformability of parasite-free RBCs from healthy mice (hRBCs) and infected mice (uRBCs) as well as corresponding spleen sizes are summarized in Fig. S1C in the supplemental material.

Influence of malaria infection and/or antimalarial drug on RBC microcirculatory behavior and splenic RBC retention. There are clear differences in the deformabilities of RBCs obtained from PVB from healthy and infected mice (Fig. 2A and B). Normalized against the average velocity of healthy RBCs (hRBCs) from healthy mice, the average velocity of uRBCs from malaria-infected mice was 0.91, 9% slower than that of hRBCs ($P < 0.001$), and the average velocity of iRBCs was only 0.58, 42% slower than that of hRBCs ($P < 0.001$). These results provide strong *in vivo* evidence that malaria parasite infections not only significantly stiffen diseased RBCs but also have a visible impact on uninfected RBCs of the host. This direct impact on uRBCs could result in an increased retention of these cells in addition to iRBCs in the spleen.

The mechanical impact of the antimalarial drug CQ on infected mice was investigated. In the peripheral blood, the average velocity of uRBCs and iRBCs dropped by 17% and 42%, respectively, after CQ treatment ($P < 0.01$) (Fig. 2C and D).

The spleen harvested from an infected mouse after 3 days of CQ treatment was 21% longer and 53% heavier than the spleen of another infected mouse receiving a PBS placebo (Fig. 2G; see

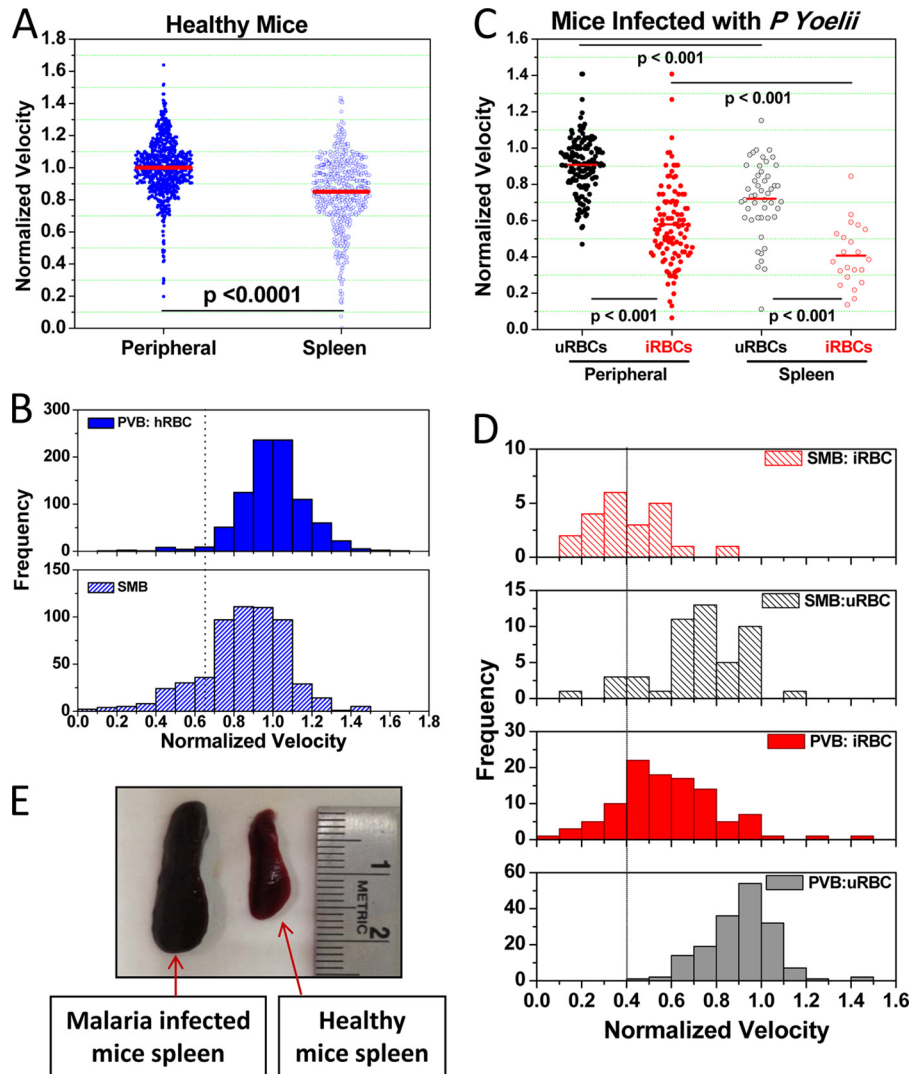


FIG 1 (A to D) Deformability of red blood cells (RBCs) extracted from SMB compared to those from PVB in both healthy (A and B) and infected (C and D) mice. In the healthy mice, the velocity of hRBCs in the spleen was significantly lower than that in peripheral blood venous blood (A) ($P < 0.0001$). Data were replotted into histograms, and a velocity threshold was then drawn at 0.65 (B). Similarly, in the infected mice, splenic iRBCs and uRBCs were significantly less deformable than corresponding peripheral blood cells ($P < 0.001$) (C). Data were replotted into histograms, and a velocity threshold of 0.40 was drawn (D). (E) Significant spleen enlargement was observed for malaria-infected mice. All deformability measurements were performed using a microfluidic device as shown in Fig. S1B in the supplemental material. Deformability data are from 6 to 9 mice per condition.

Fig. 4B and see Fig. S1C in the supplemental material). Increased spleen size and weight are typically associated with increased RBC as well as macrophage counts (17, 37). In other words, RBC congestion and retention in the red pulp could be an important contributing factor for the observed splenomegaly. This observation was in good agreement with our studies on splenic uRBC velocity (Fig. 2E and F): the average velocity of splenic uRBCs declined from 0.72 to 0.54 after CQ treatment ($P < 0.001$), and the percentage of splenic uRBCs moving at a velocity below 0.65 increased from 29% to 62% after CQ treatment, a sharp contrast to only 2.2% (19 out of 873) of untreated peripheral hRBCs that had a velocity of less than 0.65 (see Fig. S2 in the supplemental material). Details on the threshold value (0.65) determination are discussed below.

Effect of an antimalarial drug on RBC deformability profiles in peripheral blood and spleen of healthy mice. CQ was reported

to be concentrated within malaria parasites by the formation of hematin, explaining the selective drug toxicity (38). On the other hand, a high dose and/or prolonged chloroquine exposure showed detrimental effects on the spleen and brain tissues of a healthy host: significant increases in the protein and cholesterol levels were found in mice with prolonged CQ exposure, and disorganization in the red pulp was also reported (39). With our observed effect of CQ on uRBCs from *P. yoelii*-infected mice, it was interesting to investigate the effect of CQ on the deformability of hRBCs from healthy mice.

Healthy mice were treated with CQ for up to 8 consecutive days. For hRBCs sampled from PVB, the mean hRBC velocity dropped by 9% and 15%, respectively, after 4 and 6 days of consecutive CQ treatment ($P < 0.001$). No further velocity change was seen on day 9 ($P > 0.1$) (Fig. 3A). For hRBCs sampled from SMB, in addition to a gradual decrease, the velocity profile ap-

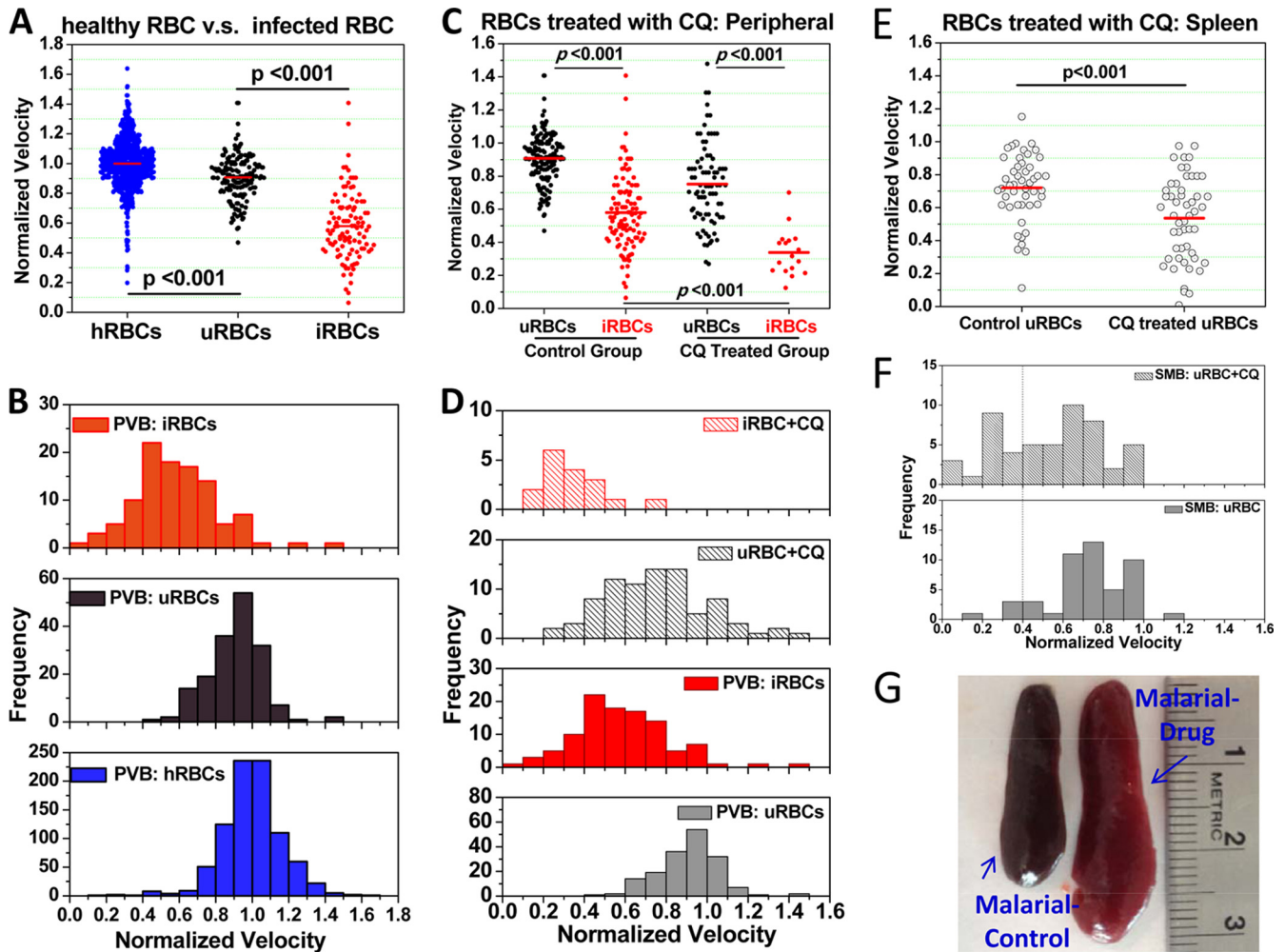


FIG 2 (A to F) Effects of malaria infection (A and B) and/or antimalarial drug treatment (C to F) on RBC deformability. RBCs were extracted from healthy mice (hRBCs) and from infected mice (uRBCs and iRBCs). The mean velocity of hRBCs is slightly higher than that of uRBCs ($P < 0.001$) and considerably higher than that of iRBCs ($P < 0.001$) (A). Data were replotted into histograms for better illustration (B). When infected mice treated with CQ, the iRBCs were found to be significantly less deformable ($P < 0.001$) (C). Data were replotted into histograms to illustrate the shift in population-wide RBC velocity (D). In the spleens of infected mice, uRBCs were also found to be significantly less deformable ($P < 0.001$) (E). A velocity threshold of 0.40 was drawn (F). Significant spleen enlargement was observed for malaria-infected mice after CQ treatment compared to infected mice treated with PBS only (G). Deformability data are from 6 to 9 mice per condition. The data for hRBCs, uRBCs, and iRBCs shown in panels A to D (control group in panels C and D) are repeated for easier comparison.

peared to assume bimodal distribution, in which two normal distributions seemed to separate at a normalized velocity close to 0.7 (Fig. 3B). Throughout the experiment, no significant size changes in the mice spleens were observed.

Bimodal estimation of splenic hRBC velocity profiles after CQ treatment. To study the distributions of hRBC velocity, Fig. 3B was replotted as histograms (see Fig. S3A in the supplemental material). We fit the data with both bimodal density functions and single normal distributions (see Fig. S3B to E in the supplemental material). A comparison of the two models via the likelihood ratio test (LRT) suggested that the bimodal distribution fit better to all SMB data ($P < 0.05$).

Since RBCs from SMB consist of two significant subpopulations of flowthrough and trapped RBCs, the contribution of each subpopulation to the overall velocity profile was assessed using probability density estimation, where a_1 denotes the fraction of cells coming from the spleen-retained population, b_1 and c_1 de-

note the mean and standard deviation of the spleen-retained RBC velocities, and b_2 and c_2 denote the mean and standard deviation of the normal RBC velocities. Parameters were estimated by the maximum-likelihood (ML) method, and all fitted results are listed in Fig. S4 in the supplemental material. The following equation was used:

$$f(x) = \sum_{i=1}^2 \left(a_i \frac{1}{\Phi\left(\frac{b_i}{c_i}\right) \sqrt{2\pi} c_i} \exp\left[-\frac{(x - b_i)^2}{2c_i^2}\right] \right)$$

where $\Phi(\cdot)$ represents the cumulative distribution function of the standard normal distribution. Based on the parametric fittings (red curves in Fig. S3 in the supplemental material), a_1 was estimated to be 0.39 in the control sample and increased to 0.68 after 6 days of consecutive CQ treatment. A CQ-induced alteration in RBC microcirculatory behavior was hence suggested by the in-

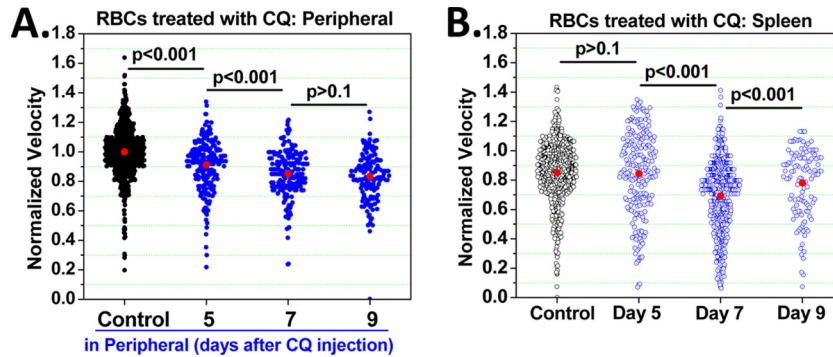


FIG 3 CQ effect on healthy RBCs *in vivo*. Whereas only a very subtle decrease in RBC deformability was observed *in vivo* in peripheral blood (A), a noticeable shift in the RBC deformability profile (from unimodal to bimodal) was demonstrated *in vivo* in splenic minced blood (B). Deformability data are from 6 to 9 mice per condition.

creased fraction of spleen-retained RBCs. Except for the control sample, the values of b_1 and b_2 remained largely unchanged, centered on 0.65 and 1.0, respectively. This result suggests a fairly constant splenic retention threshold. The value of b_2 agrees well with the average peripheral hRBC velocity of 1.0.

Malaria infection, antimalarial treatment, and blood hemoglobin concentration. Malarial anemia is one of the most common complications of *Plasmodium falciparum* malaria (20), and splenic RBC retention has been suggested to be a potential contributing mechanism (17). The possible anemic effect relating to increased splenic retention was hence investigated.

In mice infected with parasites, the average hemoglobin level had dropped from 19.3 ± 2.2 g/dl to 16.0 ± 1.3 g/dl when the parasitemia first reached 1 to 10% (Fig. 4, day 1). Infected mice were then treated with either a PBS placebo or CQ for three consecutive days. By day 4, the parasitemia of the malaria-control (i.e., PBS-treated) mice reached 50 to 90%; all displayed severe anemic syndrome with an average hemoglobin concentration of 3.8 g/dl (Fig. 4, day 4). In comparison, all malaria-drug (i.e., CQ-treated) mice had parasitemia well below 1%. Despite the very low parasite burden, the average hemoglobin concentration in these malaria-drug mice was 10.3 g/dl, still significantly lower than that on day 1 before CQ treatment (16.0 g/dl) ($P < 0.01$). It is also noted that several malaria-control mice from different experimental batches died on day 4 and were disregarded in all measurements. The death could be associated with severe anemia and therefore extremely low hemoglobin concentrations. The actual

hemoglobin concentrations in the malaria-control group were likely to be even lower.

DISCUSSION

While there have been several experimental results suggesting a significant role of splenic RBC clearance in human malaria pathology, this has never been validated in an *in vivo* setting with actual disease progression. This work aimed to study *in vivo* filtration of RBCs directly in a mouse malaria model and connect it with *in vitro* microfluidic flow cytometry-based deformability measurement. Clinical studies have shown both similarities and differences in the malaria pathology in humans and mice in terms of invasion characteristics and malarial anemia (20). For the scope of our study, which concerned mainly mechanical RBC filtration in spleen, *Plasmodium yoelii*-infected mice were chosen as our mouse model for two reasons: first, mouse spleen trapping of *Plasmodium yoelii*-infected RBCs was demonstrated by prior experimental studies (40), and second, similar to *Plasmodium falciparum* infection in humans, where the massive destruction of uninfected RBCs plays a significant role in malarial anemia, non-parasitized RBCs in *Plasmodium yoelii*-infected mice are also believed to contribute to murine malarial anemia (41). Additionally, it should be noted that for a typical nonsinusoidal spleen, adhesion (rather than deformability) is believed to be the predominant mechanism for RBC removal, as the critical mesh size of the spleen is significantly larger. However, mouse spleen has very small fenestrations (1 to 3 μm) that function mechanically like venous

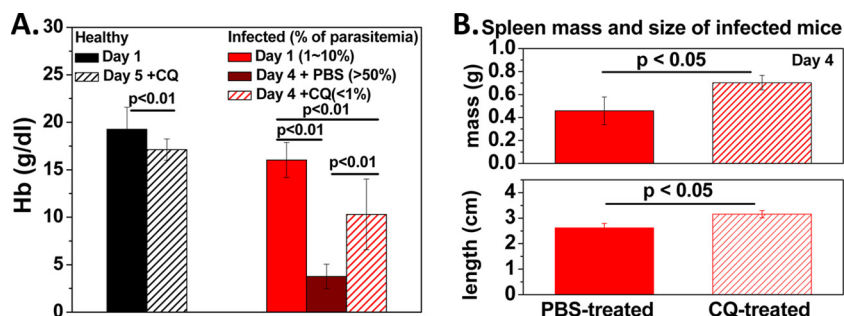


FIG 4 (A) A hemoglobin assay was performed on the venous blood extracted from healthy and malaria-infected mice. (B) Infected mice after CQ treatment exhibited significantly larger spleens in terms of mass and length ($P < 0.05$).

sinus, and RBC deformability therefore plays a major role in the splenic retention in mice (30, 31). We also note that RBC surface properties may indeed have an impact on our analysis, as well as on RBC clearance *in vivo* (42). To minimize confounding effects from RBC adhesion, we precoated the microfluidic device as well as RBC samples with 1% BSA or 20% FBS at least 20 min prior to the experiment.

It is worth mentioning that the deformability measured by a microfluidic device may not be equivalent to other measurements of cell deformability, such as by micropipette and ektacytometry. Cell deformability is a complex characteristic, depending on many factors, such as shear rate, that cannot be reduced to a single number (43). Still, our deformability cytometry is arguably better than other static deformability measurements, in terms of mimicking the splenic filtration process and predicting individual cells' filterability *in vivo*. Indeed, the percentages of most likely retained RBCs as predicted using our velocity-based single-cell measurements are in good agreement with reported retention rates of *Plasmodium falciparum* RBC cultures (16) (see Fig. S6 in the supplemental material). The relatively low shear rate ($<100\text{ s}^{-1}$) and low RBC flow velocity (up to $200\text{ }\mu\text{m/s}$) used in our system are consistent with those reported *in vivo* (44, 45), and the strong correlation between *in vitro* deformability and *in vivo* splenic filtration profile demonstrated in our data also support this argument.

RBC deformability, splenic RBC retention, and malarial anemia. Severe malarial anemia frequently is associated with high mortality rates in children and pregnant women. RBC loss is considered the primary reason. Several mechanisms were proposed to account for such massive RBC loss. Antibody-mediated hemolysis, for example, is believed to play a major role in patients with hyperreactive malaria splenomegaly. Such a delayed hemolysis effect reflects diverse pathogenic processes and is intrinsically associated with RBC deformability in two ways: on one hand, hemolysis is partly caused by a membrane defect and reduced RBC deformability, on the other hand, hemolysis affects the deformability of surrounding RBCs (46). Only recently, splenic RBC sequestration was proposed as another, simpler mechanism for RBC loss (15): less-deformable RBCs get removed through the mechanical trapping of the spleen.

In the present study, a 37.5% drop in hemoglobin concentration (from 16.0 g/dl to 10.3 g/dl) was found in the CQ-treated malarial mice, while these mice exhibited fairly low parasitemia throughout. Such a large drop cannot be attributed mainly to the hemolysis of iRBCs. On the other hand, the stiffening of uRBCs and the significant spleen enlargement after CQ treatment suggest that spleen-related removal of uRBCs may play a major role in the observed anemia. The SMB displayed a significantly lowered transit velocity (Fig. 1A and C and 2C), which is in line with the spleen filtering less-deformable RBCs. These observations, along with the earlier *ex vivo* results reported by Buffet et al. (14), establish that RBC deformability has an important contribution in *in vivo* splenic clearance.

Additionally, for the first time, we demonstrate the important links connecting RBC deformability, splenic RBC retention and malarial anemia within the *in vivo* mouse setting. Several earlier studies have raised the possibility that intensified RBC retention in spleen exacerbates malarial anemia (7, 15). Here we demonstrate that reductions in RBC deformability and increased spleen size after malaria infection and CQ treatment exhibit strong correlations with the hemoglobin concentration in the test subject. It

needs to be highlighted that CQ treatment, though it successfully reduced the parasite count in the infected mice, did not alleviate malarial anemia completely (Fig. 4), suggesting that instead of parasite loading alone, splenic retention of uRBCs could be directly responsible for the excessive blood loss in malarial anemia. The significantly lowered hemoglobin concentration (from 16.0 g/dl to 10.3 g/dl after CQ treatment) appeared to correlate with the increased size and weight of mouse spleens (Fig. 4B), which is consistent with reported clinical studies on human patients (17, 18, 22). It must be noted that our retention model is rather simplified. Splenomegaly is highly multifactorial, so knowledge about other mechanisms, such as stress erythropoiesis and immune-mediated RBC destruction, would add to the understanding of the extremely complicated and dynamic process.

Chloroquine decreases RBC deformability and enhances splenic RBC retention. Another key finding of this study is that CQ has a direct impact on the red blood cell deformability. This decrease in RBC deformability provides another mechanism of action of CQ, as it leads to increased retention of iRBCs in the spleen. On the other hand, the fact that uRBCs show reduced deformability and consequently enhanced retention in the spleen can explain the high level of anemia seen at low parasitemia levels. To the best of our knowledge, we provide here the first demonstration of CQ-induced iRBC alteration of RBC deformability *in vivo* by measuring RBC velocities under flow.

The exact mechanism for CQ-induced reduction in RBC deformability (or velocity) is still unclear. Drug-induced changes in RBC size and shape are one possible factor (47) that could have a direct impact on RBC deformability (35, 43, 48, 49). Indeed, significant changes in the size and sphericity of iRBCs (trophozoites and schizonts) were observed (see Fig. S9 in the supplemental material), and a slight increase in stomatocytes appears to be evident after 5 consecutive days of CQ treatment (see Fig. S8 in the supplemental material).

On the other hand, membrane stiffening can be another important source for drug-related iRBC rigidification, as CQ causes hemin-induced oxidative damage to the RBC membrane (46). This possibility has been validated using micropipette aspiration; the average membrane shear modulus of iRBCs (trophozoites and schizonts) was found to have increased by 2- to 8-fold after CQ treatment (see Fig. S10 in the supplemental material). The impact on uRBCs and hRBCs in both healthy and malaria-infected mice could be due to a general increase of the oxidative stress in the system (50). An earlier study in which CQ was injected into healthy Swiss mice reported that after a 5-mg/kg i.p. CQ injection (an approximately 8-fold lower dose than our 0.8 mg/mouse), both glucose-6-phosphate dehydrogenase (G6PDH) and NADH diaphorase activities of normal RBCs increased significantly (51), suggesting that the oxidative stress induced by CQ needs to be compensated for by increasing the activity of protective enzymes. On the other hand, RBCs deficient in G6PDH are more susceptible to oxidative damage, so that drug-induced oxidative stress could drastically decrease the deformability of these RBCs (52, 53). It is also possible that CQ impacts RBC deformability through accelerating hemoglobin denaturation (54). In all, the mild albeit significant reduction in hRBC and uRBC transit velocity (i.e., deformability) after CQ treatment is not unique to CQ; in a separate work, we also observed similar stiffening (in terms of both higher shear modulus and lower microcirculatory velocity) on uRBCs *in vitro*, from *Plasmodium falciparum* malaria-infected human blood

incubated with artesunate, another popular antimalarial drug containing an endoperoxide bridge (13).

Threshold prediction for splenic RBC retention. We are able to establish a clear relationship between RBC deformability and splenic RBC retention in a more quantitative manner, enabling us to study the effective threshold for retention. The term retention threshold was previously introduced (17) to describe the stringency of spleen as a mechanical filter. It was postulated that different retention thresholds may exist in healthy and malaria-infected hosts.

The average life span of red blood cells (RBCs) in BALB/c mice is approximately 40 days (55). Aged mouse RBCs, which are generally stiffer (56), are trapped by mouse spleen for phagocytosis (57). The spleen is therefore estimated to filter the least deformable 2.5% of red blood cells during microcirculation each day (17). Based on this approximation, a cutoff line was drawn in Fig. 1D, marking the bottom 2.5% of PVB. The corresponding velocity range allows a rough estimation of the splenic retention threshold in healthy animals, which is around 0.65 of the normalized PVB velocity (see Fig. S2 in the supplemental material).

This threshold is cross-validated by the maximum-likelihood parametric fitting (see Fig. S4 in the supplemental), which resolved the SMB into two potential subpopulations according to the velocity distributions. The average velocity of the spleen-retained subpopulation, as suggested by parametric fitting, is also around 0.65 (i.e., b_1) (see Fig. S4 in the supplemental material).

It is interesting to note that a shift in the retention threshold was observed in mice after malaria infection. In contrast to healthy mice, for which the threshold was estimated to be centered at 0.65 (i.e., b_1 in the equation in “Bimodal estimation of splenic hRBC velocity profiles after CQ treatment” above; see Fig. S4 in the supplemental material), malaria-infected mice seem to have a lower threshold centered at 0.4 (Fig. 2F). It is speculated that the enlargement of malarial spleen and the further spleen enlargement after CQ treatment have modified the pore size in the splenic meshwork and altered RBC microcirculation (2). A lowered spleen retention threshold could imply an enlarged pore size in malaria-infected mice, which is consistent with several independent studies (58–60) using intravital microscopy and magnetic resonance imaging, which reported dilated venous sinuses in the red pulp of enlarged spleen.

Conclusions. By employing a microfluidic single-cell deformability cytometer, we investigated the filterability or deformability of PVB and SMB from healthy and malaria-infected mice. Several interesting observations were made from the population-wide distribution of single RBC deformability. (i) RBCs extracted from SMB are less deformable than cells from PVB, suggesting that passive splenic RBC retention of less-deformable RBCs might have occurred, though the retention rate is typically low for healthy test subjects. (ii) CQ has a general stiffening effect on hRBCs, uRBCs, and iRBCs, which could result in an increased splenic RBC retention of all RBCs. The retention is evident both from RBC deformability measurement as well as spleen size quantification. It is likely that the CQ-induced alteration in RBC microcirculatory behavior is attributable to increased oxidative stress. (iii) Increased splenic RBC retention strongly corresponds to an anemic condition for both healthy and malaria-infected mice. Malarial anemia might be caused by the direct impact of intense splenic RBC retention, rather than high parasite loading. These new insights are expected to be useful in developing strate-

gies to deal with malarial anemia, which is one of the severe pathological outcomes of (chronic) malaria infection.

ACKNOWLEDGMENTS

We thank Subra Suresh for helpful discussions. Device fabrications were carried out at MIT Microsystems Technology Laboratories.

This work is supported by the National Research Foundation (Singapore) through the Singapore-MIT Alliance for Research and Technology (SMART) Center (BioSyM and ID IRG).

REFERENCES

1. Mebius RE, Kraal G. 2005. Structure and function of the spleen. *Nat. Rev. Immunol.* 5:606–616. <http://dx.doi.org/10.1038/nri1669>.
2. del Portillo HA, Ferrer M, Brugat T, Martin-Jaular L, Langhorne J, Lacerda MVG. 2012. The role of the spleen in malaria. *Cell. Microbiol.* 14:343–355. <http://dx.doi.org/10.1111/j.1462-5822.2011.01741.x>.
3. Schmidt EE, Macdonald IC, Groom AC. 1993. Comparative aspects of splenic microcirculatory pathways in mammals: the region bordering the white pulp. *Scanning Microsc.* 7:613–628.
4. Cesta MF. 2006. Normal structure, function, and histology of the spleen. *Toxicol. Pathol.* 34:455–465. <http://dx.doi.org/10.1080/01926230600867743>.
5. Schmidt EE, MacDonald IC, Groom AC. 1988. Microcirculatory pathways in normal human spleen, demonstrated by scanning electron microscopy of corrosion casts. *Am. J. Anat.* 181:253–266. <http://dx.doi.org/10.1002/aja.1001810304>.
6. Chen LT. 1978. Microcirculation of the spleen: an open or closed circulation? *Science* 201:157–159. <http://dx.doi.org/10.1126/science.663644>.
7. Buffet PA, Safeukui I, Milon G, Mercereau-Puijalon O, David PH. 2009. Retention of erythrocytes in the spleen: a double-edged process in human malaria. *Curr. Opin. Hematol.* 16:157–164. <http://dx.doi.org/10.1097/MOH.0b013e32832a1d4b>.
8. Suresh S, Spatz J, Mills JP, Micoulet A, Dao M, Lim CT, Beil M, Seufferlein T. 2005. Connections between single-cell biomechanics and human disease states: gastrointestinal cancer and malaria. *Acta Biomater.* 1:15–30. <http://dx.doi.org/10.1016/j.actbio.2004.09.001>.
9. Mills JP, Diez-Silva M, Quinn DJ, Dao M, Lang MJ, Tan KSW, Lim CT, Milon G, David PH, Mercereau-Puijalon O, Bonnefoy S, Suresh S. 2007. Effect of plasmodial RESA protein on deformability of human red blood cells harboring *Plasmodium falciparum*. *Proc. Natl. Acad. Sci. U. S. A.* 104:9213–9217. <http://dx.doi.org/10.1073/pnas.0703433104>.
10. Bow H, Pivkin IV, Diez-Silva M, Goldfless SJ, Dao M, Niles JC, Suresh S, Han J. 2011. A microfabricated deformability-based flow cytometer with application to malaria. *Lab Chip* 11:1065–1073. <http://dx.doi.org/10.1039/C0LC00472C>.
11. Diez-Silva M, Park Y, Huang S, Bow H, Mercereau-Puijalon O, Deplaine G, Lavazec C, Perrot S, Bonnefoy S, Feld M, Han J, Dao M, Suresh S. 2012. Pf155/RESA protein influences the dynamic microcirculatory behavior of ring-stage *Plasmodium falciparum* infected red blood cells. *Sci. Rep.* 2:614. <http://dx.doi.org/10.1038/srep00614>.
12. Park Y, Diez-Silva M, Popescu G, Lykotrafitis G, Choi W, Feld MS, Suresh S. 2008. Refractive index maps and membrane dynamics of human red blood cells parasitized by *Plasmodium falciparum*. *Proc. Natl. Acad. Sci. U. S. A.* 105:13730–13735. <http://dx.doi.org/10.1073/pnas.0806100105>.
13. Huang S, Undisz A, Diez-Silva M, Bow H, Dao M, Han J. 2013. Dynamic deformability of *Plasmodium falciparum*-infected erythrocytes exposed to artesunate in vitro. *Integr. Biol.* 5:414–422. <http://dx.doi.org/10.1039/c2ib20161e>.
14. Buffet PA, Milon G, Brousse V, Correas J-M, Dousset B, Couvelard A, Kianmanesh R, Farges O, Sauvanet A, Paye F, Ungeheuer M-N, Ottone C, Khun H, Fiette L, Guigon G, Huerre M, Mercereau-Puijalon O, David PH. 2006. Ex vivo perfusion of human spleens maintains clearing and processing functions. *Blood* 107:3745–3752. <http://dx.doi.org/10.1182/blood-2005-10-4094>.
15. Safeukui I, Correas J-M, Brousse V, Hirt D, Deplaine G, Mulé S, Lesurtel M, Goasguen N, Sauvanet A, Couvelard A, Kerneis S, Khun H, Vigan-Womas I, Ottone C, Molina TJ, Tréluyer J-M, Mercereau-Puijalon O, Milon G, David PH, Buffet PA. 2008. Retention of *Plasmodium falciparum* ring-infected erythrocytes in the slow, open microcirculation of the human spleen. *Blood* 112:2520–2528. <http://dx.doi.org/10.1182/blood-2008-03-146779>.

16. Deplaine G, Safeukui I, Jeddi F, Lacoste F, Brousse V, Perrot S, Biligui S, Guillotte M, Guitton C, Dokmak S, Aussilhou B, Sauvanet A, Cazals Hatem D, Paye F, Thellier M, Mazier D, Milon G, Mohandas N, Mercereau-Puijalon O, David PH, Buffet PA. 2011. The sensing of poorly deformable red blood cells by the human spleen can be mimicked in vitro. *Blood* 117:e88–e95. <http://dx.doi.org/10.1182/blood-2010-10-312801>.
17. Buffet PA, Safeukui I, Deplaine G, Brousse V, Prendki V, Thellier M, Turner GD, Mercereau-Puijalon O. 2011. The pathogenesis of Plasmodium falciparum malaria in humans: insights from splenic physiology. *Blood* 117:381–392. <http://dx.doi.org/10.1182/blood-2010-04-202911>.
18. Looareesuwan S, Ho M, Wattanagoon Y, White NJ, Warrell DA, Bunnag D, Harinasuta T, Wyler DJ. 1987. Dynamic alteration in splenic function during acute falciparum malaria. *N. Engl. J. Med.* 317:675–679. <http://dx.doi.org/10.1056/NEJM198709103171105>.
19. Chotivanich K, Udomsangpetch R, McGready R, Proux S, Newton P, Pukrittayakamee S, Looareesuwan S, White NJ. 2002. Central role of the spleen in malaria parasite clearance. *J. Infect. Dis.* 185:1538–1541. <http://dx.doi.org/10.1086/340213>.
20. Lamikanra AA, Brown D, Potocnik A, Casals-Pascual C, Langhorne J, Roberts DJ. 2007. Malarial anemia: of mice and men. *Blood* 110:18–28. <http://dx.doi.org/10.1182/blood-2006-09-018069>.
21. Dondorp AM, Angus BJ, Chotivanich K, Silamut K, Ruangveerayuth R, Hardeman MR, Kager PA, Vreeken J, White NJ. 1999. Red blood cell deformability as a predictor of anemia in severe falciparum malaria. *Am. J. Trop. Med. Hyg.* 60:733–737.
22. Price RN, Simpson JA, Nosten F, Luxemburger C, Hkijaroen L, ter Kuile F, Chongsuphajaisiddhi T, White NJ. 2001. Factors contributing to anemia after uncomplicated falciparum malaria. *Am. J. Trop. Med. Hyg.* 65:614–622.
23. Sullivan DJ, Gluzman IY, Russell DG, Goldberg DE. 1996. On the molecular mechanism of chloroquine's antimalarial action. *Proc. Natl. Acad. Sci. U. S. A.* 93:11865–11870. <http://dx.doi.org/10.1073/pnas.93.21.11865>.
24. Esposito A, Tiffert T, Mauritz JMA, Schlachter S, Bannister LH, Kaminski CF, Lew VL. 2008. FRET imaging of hemoglobin concentration in Plasmodium falciparum-infected red cells. *PLoS One* 3:3780. <http://dx.doi.org/10.1371/journal.pone.0003780>.
25. Fitch CD, Chevli R, Kanjananggulpan P, Dutta P, Chevli K, Chou AC. 1983. Intracellular ferriprotoporphyrin IX is a lytic agent. *Blood* 62:1165–1168.
26. Carlton JM, Angiuoli SV, Suh BB, Kooij TW, Pertea M, Silva JC, Ermolaeva MD, Allen JE, Selengut JD, Koo HL, Peterson JD, Pop M, Kosack DS, Shumway MF, Bidwell SL, Shallom SJ, van Aken SE, Riedmuller SB, Feldblyum TV, Cho JK, Quackenbush J, Sedegah M, Shoaibi A, Cummings LM, Florens L, Yates JR, Raine JD, Sinden RE, Harris MA, Cunningham DA, Preiser PR, Bergman LW, Vaidya AB, van Lin LH, Janse CJ, Waters AP, Smith HO, White OR, Salzberg SL, Venter JC, Fraser CM, Hoffman SL, Gardner MJ, Carucci DJ. 2002. Genome sequence and comparative analysis of the model rodent malaria parasite Plasmodium yoelii yoelii. *Nature* 419:512–519. <http://dx.doi.org/10.1038/nature01099>.
27. Negreiros RM, Makimoto FH, Santana LL, Ferreira LC, Nakajima GS, Santos MC. 2009. Experimental splenectomies and malaria in mice. *Acta Cir. Bras.* 024:437–441. <http://dx.doi.org/10.1590/S0102-86502009000600003>.
28. Bapat D, Huang X, Gunalan K, Preiser PR. 2011. Changes in parasite virulence induced by the disruption of a single member of the 235 kDa rhoptry protein multigene family of Plasmodium yoelii. *PLoS One* 6:20170. <http://dx.doi.org/10.1371/journal.pone.0020170>.
29. Stutte HJ. 1968. Nature of human spleen red pulp cells with special reference to sinus lining cells. *Cell Tissue Res.* 91:300–314.
30. Hataba Y, Kirino Y, Suzuki T. 1981. Scanning electron microscopic study of the red pulp of mouse spleen. *J. Electron Microsc.* 30:46–56.
31. Klausner MA, Hirsch LJ, Leblond PF, Chamberlain JK, Klemperer MR, Segel GB. 1975. Contrasting splenic mechanisms in the blood clearance of red blood cells and colloidal particles. *Blood* 46:965–976.
32. Lewis M, Pfeil J, Mueller A-K. 2011. Continuous oral chloroquine as a novel route for Plasmodium prophylaxis and cure in experimental murine models. *BMC Res. Notes* 4:262. <http://dx.doi.org/10.1186/1756-0500-4-262>.
33. Hagihara N, Walbridge S, Olson AW, Oldfield EH, Youle RJ. 2000. Vascular protection by chloroquine during brain tumor therapy with Tf-CRM107. *Cancer Res.* 60:230–234.
34. Young LE, Platzer RF, Ervin DM, Izzo MJ. 1951. Hereditary spherocytosis. *Blood* 6:1099–1113.
35. Safeukui I, Buffet PA, Deplaine G, Perrot S, Brousse V, Ndour A, Nguyen M, Mercereau-Puijalon O, David PH, Milon G, Mohandas N. 2012. Quantitative assessment of sensing and sequestration of spherocytic erythrocytes by the human spleen. *Blood* 120:424–430. <http://dx.doi.org/10.1182/blood-2012-01-404103>.
36. Murphy SC, Fernandez-Pol S, Chung PH, Prasanna Murthy SN, Milne SB, Salomao M, Brown HA, Lomasney JW, Mohandas N, Haldar K. 2007. Cytoplasmic remodeling of erythrocyte raft lipids during infection by the human malaria parasite Plasmodium falciparum. *Blood* 110:2132–2139. <http://dx.doi.org/10.1182/blood-2007-04-083873>.
37. Fudenberg H, Baldini M, Mahoney JP, Dameshek W. 1961. The body hematocrit/venous hematocrit ratio and the “splenic reservoir”. *Blood* 17:71–82.
38. Macomber PB, Sprinz H, Tousimis AJ. 1967. Morphological effects of chloroquine on Plasmodium berghei in mice. *Nature* 214:937–939. <http://dx.doi.org/10.1038/214937a0>.
39. Desai KR, Dattani JJ, Rajput DK, Moid N, Yagnik BJ, Highland HN, George LB. 2010. Effect of chronic administration of chloroquine on the gastrocnemius muscle, spleen and brain of Swiss albino mice. *Asian J. Trad. Med.* 5:62–69.
40. Smith LP, Hunter KW, Oldfield EC, Strickland GT. 1982. Murine malaria: blood clearance and organ sequestration of Plasmodium yoelii-infected erythrocytes. *Infect. Immun.* 38:162–167.
41. Totino P, Magalhaes A, Silva L, Banic D, Daniel-Ribeiro C, Ferreira-da-Cruz M. 2010. Apoptosis of non-parasitized red blood cells in malaria: a putative mechanism involved in the pathogenesis of anaemia. *Malaria J.* 9:350. <http://dx.doi.org/10.1186/1475-2875-9-350>.
42. Low P, Waugh S, Zinke K, Drenckhahn D. 1985. The role of hemoglobin denaturation and band 3 clustering in red blood cell aging. *Science* 227:531–533. <http://dx.doi.org/10.1126/science.2578228>.
43. Chien S. 1987. Red cell deformability and its relevance to blood flow. *Annu. Rev. Physiol.* 49:177–192. <http://dx.doi.org/10.1146/annurev.ph.49.030187.001141>.
44. MacDonald IC, Schmidt EE, Groom AC. 1991. The high splenic hematocrit: a rheological consequence of red cell flow through the reticular meshwork. *Microvasc. Res.* 42:60–76. [http://dx.doi.org/10.1016/0026-2862\(91\)90075-M](http://dx.doi.org/10.1016/0026-2862(91)90075-M).
45. MacDonald IC, Ragan DM, Schmidt EE, Groom AC. 1987. Kinetics of red blood cell passage through interendothelial slits into venous sinuses in rat spleen, analyzed by in vivo microscopy. *Microvasc. Res.* 33:118–134. [http://dx.doi.org/10.1016/0026-2862\(87\)90011-2](http://dx.doi.org/10.1016/0026-2862(87)90011-2).
46. Nuchsongsin F, Chotivanich K, Charunwathana P, Fausta O-S, Taramelli D, Day NP, White NJ, Dondorp AM. 2007. Effects of malaria heme products on red blood cell deformability. *Am. J. Trop. Med. Hyg.* 77:617–622.
47. Glaser R. 1979. The shape of red blood cells as a function of membrane potential and temperature. *J. Membr. Biol.* 51:217–228. <http://dx.doi.org/10.1007/BF01869085>.
48. Safeukui I, Buffet PA, Perrot S, Sauvanet A, Aussilhou B. 2013. Surface area loss and increased sphericity account for the splenic entrapment of subpopulations of Plasmodium falciparum ring-infected erythrocytes. *PLoS One* 8:60150. <http://dx.doi.org/10.1371/journal.pone.0060150>.
49. Reinhart WH, Chien S. 1986. Red cell rheology in stomatocyte-echinocyte transformation: roles of cell geometry and cell shape. *Blood* 67:1110–1118.
50. Iyawe HOT, Onigbinde AO. 2004. Effect of an antimalarial and a micronutrient supplementation on respiration induced oxidative stress. *Pakistan J. Nutr.* 3:318–321. <http://dx.doi.org/10.3923/pjn.2004.318.321>.
51. Bhatia ACP. 1985. Chloroquine induces oxidative lysis of Plasmodium berghei parasitized red blood cells. *Ann. Soc. Belg. Med. Trop.* 65(Suppl 2):97–103.
52. Liu TZ, Lin TF, Hung IJ, Wei JS, Chiu D. 1994. Enhanced susceptibility of erythrocytes deficient in glucose-6-phosphate dehydrogenase to alloxan/glutathione-induced decrease in red cell deformability. *Life Sci.* 55:55–60.
53. Chiu D, Liu T. 1997. Free radical and oxidative damage in human blood cells. *J. Biomed. Sci.* 4:256–259. <http://dx.doi.org/10.1007/BF02253426>.
54. Fitch CD, Russell NV. 2006. Accelerated denaturation of hemoglobin and the antimalarial action of chloroquine. *Antimicrob. Agents Chemother.* 50:2415–2419. <http://dx.doi.org/10.1128/AAC.01652-05>.

55. Horký J, Znojil V. 1978. Comparison of life span of erythrocytes in some inbred strains of mouse using ¹⁴C-labelled glycine. *Physiol. Bohemoslov.* 27:209–217.
56. Waugh RE, Narla M, Jackson CW, Mueller TJ, Suzuki T, Dale GL. 1992. Rheologic properties of senescent erythrocytes: loss of surface area and volume with red blood cell age. *Blood* 79:1351–1358.
57. Mohandas N, Gallagher PG. 2008. Red cell membrane: past, present, and future. *Blood* 112:3939–3948. <http://dx.doi.org/10.1182/blood-2008-07-161166>.
58. Freitas CRL, Barbosa AA, Jr, Fernandes A, Andrade ZA. 1999. Pathology of the spleen in hepatosplenic schistosomiasis. Morphometric evaluation and extracellular matrix changes. *Mem. Inst. Oswaldo Cruz* 94:815–822.
59. Ferrer M, Martin-Jaular L, Calvo M, del Portillo HA. 2012. Intravital microscopy of the spleen: quantitative analysis of parasite mobility and blood flow. *J. Vis. Exp.* 59:3609. <http://dx.doi.org/10.3791/3609>.
60. Bae K, Jeon KN. 2006. CT findings of malarial spleen. *Br. J. Radiol.* 79:145–147. <http://dx.doi.org/10.1259/bjr/46185784>.